Published in final edited form as:
J Neuropathol Exp Neurol. 2010 October ; 69(10): 1078–1085. doi:10.1097/NEN.0b013e3181f530ec.

Early or Late-Stage Anti-N-Terminal Huntingtin Intrabody Gene Therapy Reduces Pathological Features in B6.HDR6/1 Mice

Abigail Snyder-Keller, PhD[a,b,c], **Julie A. McLear, PhD**[a,d], **Tyisha Hathorn, MS**[c], and **Anne Messer, PhD**[a,b,c]

[a]Wadsworth Center, NY State Dept. of Health, Albany, New York

[b]Department of Biomedical Sciences, School of Public Health, University at Albany, Albany, New York

[c]Center for Neuropharmacology and Neuroscience, Albany Medical College, Albany, New York

Abstract

Huntington disease (HD) is a progressive neurodegenerative disease caused by an expansion of a polyglutamine sequence in mutant huntingtin (mhtt) that produces abnormal folding and aggregation that results in the formation of nuclear and cytoplasmic neuronal inclusion bodies. Although the precise role of mhtt aggregates in the pathogenesis is unclear, attempts to reduce accumulated mhtt protein have ameliorated the phenotype in multiple cellular and in vivo HD models. Here, we provide critical results on intracranial delivery of a single-chain Fv intrabody, C4, which targets the first 17 amino acids of the htt protein, a region of httExon1 that is increasingly being recognized as pivotal. To assess long-term efficacy and safety issues, we used adeno-associated viral vectors (AAV2/1) to deliver intrabody genes to striatum of inbred B6.HDR6/1 mice. Treatment initiation at various stages of the disease showed that early treatment preserved the largest number of cells without nuclear aggregates and that the accumulation of aggregated material could be delayed by several months. Even when intrabody treatment was not initiated until the clinical disease stage, significant, albeit smaller, effects were seen. These data indicate that neuronal intrabodies against critical N-terminal epitopes can be safely and effectively delivered using AAV2/1 to delay the aggregation phenotype over a sustained period of time in this HD model, even when delivery is initiated after disease onset.

Keywords

AAV; Aggregates; Gene therapy; Huntington disease; Intrabody; R6/1 mice; scFv

Introduction

Huntington disease (HD) is one of a group of neurodegenerative disorders linked to abnormally high numbers of trinucleotide repeats in the defective gene (1). The mutant huntingtin protein (mhtt), which contains an elongated polyglutamine sequence (>37 CAG repeats), undergoes abnormal folding, proteolytic cleavage to N-terminal fragments, and aggregation to form neuronal inclusion bodies (2,3). Aggregates of mhtt are found throughout the brain but they are particularly concentrated in the striatum and cortex, regions that incur significant cell dysfunction and loss (4). Although the role of mhtt

Correspondence and reprint requests to: Abigail Snyder-Keller, Wadsworth Center, NY State Dept. of Health, 120 New Scotland Ave., Albany, NY 12208. ph: 518-402-2623; FAX: 518-402-2457; snykell@wadsworth.org.
[d]Present address: Dept. of Biology, Utica College, 1600 Burrstone Rd., Utica, NY 13502.

aggregates in the pathogenesis remains a focus of much debate, attempts to reduce buildup of mhtt have yielded favorable outcomes on a number of measures (5-7).

Transgenic mouse models of HD (e.g. HDR6/2 and HDR6/1 mice) in which exon 1 of the huntingtin gene contains a stretch of approximately 160 and 125 CAG repeats, respectively, recapitulate the process of mhtt accumulation and aggregate formation (8,9). The more commonly studied R6/2 mice exhibit nuclear and neuropil aggregates of mhtt very early in life, and have greatly shortened lifespans. R6/1 mice exhibit a more prolonged pathogenic time course; nuclear expression of the mutant protein is demonstrable within 4 weeks after birth, and mhtt aggregates are present by 10 weeks (10,11). Coincident with increases in the frequency and size of the aggregates, HD mice begin to lose weight relative to their wild-type (wt) littermates and eventually display motor deficits and undergo premature death (9).

We have developed intracellularly expressed single-chain Fv (scFv) antibodies (intrabodies) as an approach to prevent or slow the process of aggregate formation. By binding to mhtt, targeted intrabodies can reduce toxicity in a variety of ways (12). One such intrabody, C4, is directed against the first 17 amino acids of the N-terminal fragment of mhtt. In cellular models, co-transfection of mhtt Exon1 with 75-95 CAG repeats plus scFv C4 reduced the formation of aggregates as well as cellular toxicity (13-15). Moreover, scFv-C4 reduced neurodegeneration and aggregate formation, and prolonged lifespan in Drosophila expressing mhtt Exon 1-92Q, (16).

Initial attempts at delivery into HD mice utilized the equine infectious anemia virus to effect transduction and stable expression of scFv-C4 in the forebrain (10,14). Here, we here used recombinant adeno-associated viral vectors (AAV2/1) to deliver the scFv C4 to the striatum of inbred B6.R6/1 mice before or after the development of aggregates and clinical signs. After short and long survival times, brains were analyzed for the spread of the virus, efficiency of transduction, and ability of the C4 intrabody to reduce mhtt aggregate formation in striatal neurons on a cellular basis.

Materials and Methods

AAV2/1 scFv-C4 Preparation

The scFv-C4 gene, fused to a hemagglutinin (HA) tag, was cloned into an AAV2 shuttle vector, as previously described (17), and transferred to the University of Iowa Vector core, under the direction of Dr. B. Davidson, for vector production using the helper-free HEK293 triple transfection method (Stratagene, La Jolla, CA) with an AAV1 capsid. Vector was purified, titered, and used at the concentrations indicated below.

Animals

B6.HD6/1 is a C57BL6/J congenic substrain of the original HDR6/1, harboring httExon1 plus approximately 1 kb of upstream regulatory DNA. The congenic line was established, and is maintained, at the Wadsworth Center by breeding transgenic males to C57BL6/J females; CAGs = 120-125. The strain has also been transferred to the Jackson Laboratory (Bar Harbor, ME) for general distribution (Jax # 000664). Offspring were genotyped by PCR from tail biopsy. All animal procedures were approved by the Wadsworth Center Institutional Animal Care and Use Committee.

At 5 to 24 weeks of age, male B6.HDR6/1 mice and wt littermates received a stereotactic injection of anti-htt scFv-C4 into the left striatum. Under isoflurane anesthesia, 2 μl of AAV2/1 anti-htt scFv-C4 (10e12 Vg/ml) were delivered at 0.22 μl/min with a syringe pump, at the following coordinates: A+1.0, L+2.1 (or +2.0 for 5-week-old mice), V-2.8, 2.6 and 2.4 (0.66 μl at each depth). The needle remained in place for 4 minutes prior to slow

withdrawal; 2 μl of saline were delivered to the contralateral striatum. The incision was closed with 5-0 sutures, and the mice recovered on a heating pad. After surgery, the mice were housed at no more than 3 per cage with littermates and were weighed once per week.

Tissue processing and immunohistochemistry

At specified survival times, anesthetized mice were perfused with warm phosphate-buffered saline (PBS), followed by cold 4% paraformaldehyde in 0.1 M phosphate buffer (PB). Brains were removed and placed in the same fixative for 20 hours, and then transferred to 15% sucrose in 0.1M PB for at least 8 hours. Thirty-μm-thick sections were cut frozen on a sliding microtome and collected in 0.1M PB. For analysis of the time course of aggregate development, brains from uninjected B6.HD6/1 mice were fixed in Bouin's fixative, embedded in paraffin, and sectioned at 5 μm. Sections were deparaffinized and rehydrated through a descending alcohol series for immunohistochemistry (IHC) for EM48.

Intrabody was visualized by IHC for the HA tag. Selected sections were rinsed in PBS and then pre-incubated in 0.2% Triton X-100 in PBS containing 5% normal goat serum. Sections were then incubated, free-floating, for 18 hours at 4°C in anti-HA polyclonal antibodies (Santa Cruz Biotechnology, Santa Cruz, CA; 1:500) in 0.1% Triton/2.5% serum/PBS. After rinsing in PBS, sections were incubated in biotinylated goat anti-rabbit secondary antibodies for 1 hour, rinsed again, and then transferred to a solution of avidin-biotin complex linked to peroxidase (Elite ABC kit, Vector Labs, Burlingame, CA). After rinsing, antibody binding was revealed with a final incubation in 0.05% diaminobenzidine containing 0.25% nickel ammonium sulfate and 0.0015% H_2O_2. Sections were mounted onto slides coated with chrom-alum gelatin, dehydrated, and coverslipped with Permount.

Additional antibodies used were: EM48 (mouse monoclonal; Millipore; Temecula, CA; 1:250) or S830 (sheep polyclonal anti-mhtt; gift of G. Bates, London; 1:5000) to stain for mhtt; anti-parvalbumin (Sigma; St. Louis, MO; 1:1000) and anti-neuronal nitric oxide synthase (nNOS, Millipore; 1:1000), to reveal striatal interneuron subtypes; anti-NeuN (Millipore; 1:500) for neurons; anti-glial fibrillary acidic protein (GFAP, Sigma; 1:500) and Iba-1 (anti-microglia-specific calcium binding protein, Wako; Richmond, VA; 1:1250), for glial subtypes. The EM48 antibody has previously been shown to preferentially label mhtt in both mouse (18) and human HD brain tissue (4). Single-label IHC was performed as above, with the appropriate secondary antibodies and normal horse serum used in place of normal goat serum when using primary antibodies made in mouse. Controls for nonspecific staining were carried out with each assay by omission of the primary antibody. Stained sections were examined and imaged on an Olympus BX60 microscope.

Double-label fluorescence

On the basis of the IHC used to reveal the full spread of the injected AAV-intrabody, sections were chosen for double-label fluorescence from regions in which striatal transduction was most extensive. Sections were first stained with EM48 or S830 overnight at 4°C followed by Alexa 594-conjugated anti-mouse or anti-sheep antibodies (Invitrogen; Eugene, OR; 1:200 for 2 hours at room temperature) and then incubated in anti-HA primary antibodies, followed the next day by Alexa 488-conjugated anti-rabbit antibodies. Sections were mounted onto slides and coverslipped with Vectashield with DAPI (Vector Labs). A Zeiss Axioskop2 microscope was used to collect images at wavelengths optimized for green (Alexa 488) and red (Alexa 594) fluorescence the images were superimposed using OpenLab software. Representative cells from selected mice were imaged by confocal microscopy to confirm colocalization (data not shown).

Quantification of AAV spread and aggregates

To determine the extent of spread of the AAV2/1 anti-htt scFv-C4, every twelfth section through the striatum was stained for the HA tag by immunoperoxidase. In each section, both the striatum and the striatal region containing HA-immunoreactivity (-IR) were outlined using NIH ImageJ, and the area of spread calculated as the quotient of the latter area over the former. The limits of the AAV spread in the rostral-caudal dimension were defined as the sections in which the HA-IR represented less than 10% of the striatal area.

For determination of the presence of mhtt aggregates in transduced and non-transduced cells, HA-IR fluorescent cells were identified in each of dorsal, medial, lateral, and ventral quadrants of striatum. In each quadrant, sampling consisted of 10 cells identified as being intensely HA+ and 10 cells with no HA-IR (the latter identified by switching to the DAPI channel). By switching to the red fluorescence, we determined the presence of mhtt aggregates (EM48 staining) for each cell. When an aggregate was present but was noticeably smaller than those in non-transduced cells in the vicinity, it was designated as a 'small' aggregate; these were later verified to be less than 2.1 μm in diameter vs. 2.2-3.4 μm for 'large' aggregates. An additional 10 cells in each of the 4 quadrants were identified in the contralateral striatum (saline-injected) by DAPI, and the presence of EM48-immunoreactive aggregates was recorded. For each animal the percentage of transduced cells containing aggregates was calculated (#/40), as well as the percentage containing large aggregates. Because non-transduced cells in the ipsilateral striatum were no different from cells in the contralateral striatum, they were combined.

Results

Intrastriatal injections of AAV2/1 scFv-C4 produce robust expression of C4 in both young and old B6.HDR6/1 and wt mouse brains

At all ages, HA-IR indicating scFv-C4 expression was present in up to 90% of the striatal area in individual sections, and spanning 800-1500 μm in the rostral-caudal dimension (Fig. 1). HA-IR cells varied in terms of the intensity of staining; intensely stained cells (roughly 30%) were distributed randomly within a zone of lightly labeled cells. Numerous transduced neurons were evident as early as 2 weeks after injection; the extent of spread and percentage of transduced neurons persisted for at least 6 months, the longest survival time examined. No differences were observed between HD and wt mice with respect to spread of the virus or numbers of cells transduced (Fig. 1A, B vs. C, D). Importantly, injections into older mice produced spread and transduction of neurons comparable to that seen in younger mice (Fig. 1E-H). At 16 to 24 weeks, pathological changes in striatum have begun and intranuclear aggregates are clearly present in a majority of neurons (Fig. 1I-L).

Double-label immunofluorescence for HA and NeuN revealed that transfected cells were indeed neurons (Supplementary Fig. 1A, D). Double labeling with antibodies to nNOS and parvalbumin demonstrated that AAV2/1 did transduce some parvalbumin-IR interneurons (Supplementary Fig. 1B, E), but not any nNOS+ interneurons (Supplementary Fig. 1C, F). Double labeling for scFv-C4 and either GFAP (for astrocytes) or Iba-1 (for microglia) revealed that few glia were immunoreactive for the transfected construct (data not shown).

scFv-C4 expression reduces the size and frequency of mhtt aggregates in striatal neurons after AAV2/1 scFv-C4 injections into B6.HDR6/1 mouse striatum

B6.HDR6/1 mice develop mhtt aggregates by 10 weeks of age, which increase in size and frequency over the next 6 to 10 weeks (Fig. 1I-L) (11). By 16 weeks, approximately 85% of striatal neurons exhibit what was designated as "large" aggregates (because the sizes did not appear to increase beyond that age). By 20 weeks this proportion increased to 98%-100%.

To examine whether transduction with AAV2/1 scFv-C4 altered the development or persistence of mhtt aggregates when the intrabody was introduced prior to aggregate formation, we analyzed the brains of mice injected at 5 to 8 weeks of age. Double-label immunofluorescence was performed for scFv-C4 (using the HA tag) and mhtt (EM48 antibody). Transduced cells were separated into intensely and weakly HA+ cells; neighboring non-transduced cells were identified by DAPI labeling. Analysis of mhtt aggregates in transduced striatal cells in mice injected at 5 to 8 weeks and killed at 16 to 32 weeks of age revealed the presence of scFv-C4-containing cells that had smaller aggregates, or no aggregates (Fig. 2A-D).

Quantification of the presence of aggregates in the intensely labeled transduced cells revealed a reduction at all ages examined, when compared to the presence of aggregates in non-transduced cells, either on the injected side or in the contralateral striatum (Fig. 2E). This reduction was particularly dramatic when only large aggregates were considered. For example, in mice killed at 16 weeks of age, 50.8% of transduced neurons had aggregates vs. 95% of non-transduced cells. Only 7.4% of cells expressing scFv-C4 contained large aggregates vs. 85% of non-transduced cells. When nearly all striatal neurons contain large aggregates in B6.HDR6/1 mice, (at 20 weeks of age or older), only 22% of cells expressing scFv-C4 (average of 10 mice) contained large aggregates. The overall percentage of transduced cells with aggregates (large and small combined) was 70%, indicating that although many of the intrabody-expressing cells still contained aggregates, these aggregates were in general smaller than those found in non-transduced neurons. ANOVA revealed a significant interaction between age at death and the presence of intrabody on the incidence of aggregates, indicating that as the mice age, the aggregates continue to develop, albeit at a reduced rate.

To determine whether the C4 intrabody slowed aggregate formation when it was introduced at ages beyond the time when aggregates appear, we delayed the AAV2/1 scFv-C4 injection until 10 to 24 weeks of age. At these older ages, the efficiency of viral transduction was comparable to that seen at younger ages in terms of the degree of spread and the percentage of transduced neurons (Fig. 2F-I). Although aggregates were still present in over 75% of transduced neurons, half of such neurons contained aggregates that were smaller than aggregates present in non-transduced neurons. The incidence of large aggregates in non-transduced neurons, either in the vicinity of the injection site or in the contralateral striatum, was 98% (Fig. 2J).

Quantification of the presence and size of aggregates as a function of age of injection revealed a main effect of scFv-C4 across all ages (including mice injected at 5-8 weeks). In mice injected at 10 to 12 weeks of age and killed 8 to 10 weeks after the injection, the efficacy of the intrabody was only slightly reduced compared to injections made at 5 to 8 weeks: 75% of scFv-C4-expressing cells had aggregates, with 33% containing large aggregates (Fig. 2J). Even after injections at 16 to 24 weeks of age, the percentage of scFv-C4-expressing striatal neurons that still contained large aggregates was reduced (average of less than 60% compared to 98-100%), and the percentage of intrabody-expressing neurons with aggregates was 75%-87%, which is still less than the 95-100% incidence of aggregates in non-transduced striatal neurons at the age at which the injections were done (Fig. 2J). Thus, despite the fact that the efficacy of the intrabody was reduced relative to the efficacy of injections made in younger animals, the intrabody still induced aggregate reduction in 40%-50% of striatal neurons that were transduced after AAV2/1 injection.

AAV2/1 scFv-C4 is well tolerated by the mice and produces little glial reaction around the injection site

To assess toxicity of the AAV2/1 and/or intrabody, we examined the brains at various times post-injection, using antibodies for astrocytes (GFAP) and microglia (Iba-1). A modest glial reaction at the injection site was revealed by GFAP IHC (Supplemental Fig. 2A-D). This was most noticeable at early times after the injection, and dissipated with time, such that at survival times longer than 4 weeks modest glial reactivity remained only at the immediate site of injection (Supplemental Fig. 2A, C, D), and was no greater than that present in the contralateral striatum after saline injection (Supplemental Fig. 2B). Few activated microglia, as determined by the rounded-up rather than ramified morphology of Iba-1-IR cells, were present, and only in the immediate vicinity of the needle track (Supplemental Fig. 2E-G). Similar numbers were also present after saline injection (Supplemental Fig. 2H). Importantly, no differences were observed between HD and wt mice in terms of activated glial reaction to the injection (compare panels C to D for GFAP and panels F to G for Iba-1), and no greater increase in glial reactivity was observed after injections into older mice (compare panels C and D to A for GFAP, and panels F and G to E for Iba-1).

B6.HDR6/1 mice injected with C4 intrabody exhibited a body weight change over time that was similar to that seen in B6.HDR6/1 mice not receiving intrabody (data not shown); this indicates an absence of either toxic or overtly beneficial effects of these unilateral intrastriatal injections on the overall health of the mice.

Discussion

Aggregates of mhtt are a neuropathological feature of the human HD brain (3,4) and occur in most cell and in vivo mouse models of HD (8,19,20). The question of whether the formation of aggregates or intranuclear inclusions of mhtt is the underlying pathological event or a protective mechanism invoked by the cell remains a matter of active debate. Buildup of the defective protein in the nucleus appears to be required for mhtt to exert toxic effects on the cell. In cellular models, the addition of a nuclear export signal to mhtt prevents the neurodegeneration associated with mhtt expression (21). However, evidence has accrued that demonstrates that visible inclusion body formation reduces levels of mhtt and neuronal death (21,22). As originally proposed by Morton et al (19), aggregate formation could be a biphasic event, with the initial formation of intranuclear inclusions serving to sequester mhtt and protect the cell; later, further growth of the inclusions leads to cellular stress that eventually results in death of the cell. In that context, the ability of therapeutic agents to limit the growth rate of the intranuclear inclusions may provide the greatest benefit.

Intracellular antibody fragments, or intrabodies, offer a proteomic approach to treatment of misfolding, aggregating proteins. We proposed that anti-htt intrabodies would exhibit cellular protection and the ability to reduce aggregation of mhtt (10,12). After examining several intrabodies directed at various domains of htt, we obtained the most dramatic amelioration of cellular dysfunction with the scFv-C4, directed against the first 17 aa, in both cellular and Drosophila HD models (13-16). For evaluation of its in vivo efficacy in a mammalian model, we chose R6/1 mice. In view of their extended life span compared to that of R6/2 mice, the use of this strain permits analysis of the efficacy of the intrabody at various stages of the disease.

Delivery of the intrabody prior to the first appearance of mhtt aggregates was most effective; animals injected at 5 to 8 weeks of age had dramatic reductions in the presence of large aggregates within transduced striatal neurons. However, the C4 intrabody was still effective when it was injected at the time mhtt aggregates are forming in this strain (10-12 weeks).

Even when injected at an age when large aggregates are present in nearly all striatal neurons (16-24 weeks), the C4 intrabody appeared to partially reverse the process whereby mutant htt is incorporated into aggregates. This reversal could be explained by the prevention of additional mhtt formation allows the cell to begin to clear the aggregated protein, as demonstrated previously by Yamamoto et al using a conditional transgenic mouse model (23). Exactly how intrabodies interact with the mutant protein and accelerate the process of degradation remains to be elucidated. Longer survival times do not result in greater reductions in mhtt aggregates; instead, maximal efficacy seems to be achieved at 10 to 16 weeks after the injection in animals killed by 22 weeks of age. The incidence of aggregates, or the presence of larger aggregates, appeared to be higher in animals sacrificed at later time points.

The use of AAV transduction of the genes for anti-mhtt intrabodies permits the long-term synthesis of these potential therapeutics. Wang et al delivered an intrabody targeting mhtt (EM48) by an adenoviral vector into R6/2 and N171-82Q mice, and found a reduction of neuropil aggregates, but no reduction in the larger nuclear aggregates (also known as nuclear inclusions) (24). Southwell, Ko and Patterson performed extensive analyses of the efficacy of 2 different intrabodies in 4 transgenic HD mouse lines, as well as after lentiviral delivery of mhtt (25). Both intrabodies reduced the presence of mhtt aggregates in the neuropil, and one of them, Happ1, (which gains access to the nucleus), reduced the presence of nuclear inclusions within the transduced region. Interestingly, the greatest behavioral improvement was found in mice treated with Happ1, suggesting that targeting of the intranuclear aggregates is of the greatest benefit.

Our present findings relate to 3 critical issues in the intrabody field. First, our intrabody is directed against the first 17 aa of the htt protein, a domain that has been increasingly identified as a critical region for modification of the function of mhtt (26). Alteration of the charge and/or intracellular localization of the target should induce specific effects on the pathogenicity. Second, for the purposes of developing a clinically relevant intrabody protocol, it is important to evaluate the interaction of the intrabody, as well as the AAV used for delivery, with the host tissue at various stages of the pathogenic process. Because the R6/1 mouse is characterized by an extended time course of pathological progression and behavioral manifestations and exhibits intranuclear aggregates of the mutant protein, the expanded time course in this model allowed us to assess the efficacy of intrabody treatment at various stages of the disease. Finally, our method for counting aggregates involved a cell-by-cell assessment driven by the presence of intrabody expression in individual transduced cells rather than the examination of aggregate frequency in the area of AAV spread. Our results suggest that intrabody efficacy varies on a cell-by-cell basis, depending on the amount of intrabody expressed. Further studies will be necessary to determine whether any variations observed reflect differences in the number of viral copies delivered to individual neurons. In addition, with the use of bilateral injections we will be able to determine the full efficacy of these intrabodies in terms of behavioral improvements.

AAV has been used extensively to deliver genes intracranially. In particular, AAV2 exhibits a strong preference for neuronal transduction (27-29). Greater spread has been observed with AAV1 (30), and packaging of AAV2 into the AAV1 capsid increases dissemination of the virus (31). In our hands, the delivery of scFv-C4 by AAV2/1 injection into the striatum produced robust transduction of neurons in a zone extending about 1 mm radially from the injection site. Although the vast majority of transduced cells in the striatum are expected to be GABA-containing medium spiny projection neurons, we found that parvalbumin+, but not nNOS+ neurons were occasionally transduced. That is of interest because of the known susceptibility of the parvalbumin interneurons in HD (32), whereas nNOS-containing neurons are spared (33).

In summary, we have shown that intracellular targeting of the first 17 aa of mhtt, using an intracellular antibody fragment can effectively counteract the aggregation phenotype in transduced cells in a transgenic mouse model of HD. Methods to increase the fraction of cells transduced, the spread of the viral vectors, and the efficacy of the intrabody protein production in transduced cells are the subject of intensive investigation in the field of neural gene therapy. Combinatorial therapies that include optimized viral vectors delivering intrabodies that bind specific targets within the mutant protein, along with the use of small molecule drugs that can act systemically, offer the most promising approach to effective therapeutics (34).

Supplementary Material

Refer to Web version on PubMed Central for supplementary material.

Acknowledgments

We thank Kevin Manley for expert assistance with the statistical analyses, Lizbeth Day for HD mouse assistance, and Dr. Erik Kvam and other members of the Messer lab for valuable discussions and suggestions. The Wadsworth Center Histopathology Core provided paraffin sections, and the confocal microscope in the Advanced Light Microscopy Core was used to confirm double labeling.

This work was supported by NIH/NINDS to A.M. (NS053912), and a graduate student diversity supplement (to NS053912) to T.H. The Univ. Iowa Vector core, Beverly Davidson, Ph.D., director, is supported by NIH/NIDDK and the Roy J Carver Trust.

References

1. La Spada AR, Taylor JP. Repeat expansion disease: progress and puzzles in disease pathogenesis. Nat Rev Genet. 2010; 11:247–58. [PubMed: 20177426]
2. Group THsDCR. A novel gene containing a trinucleotide repeat that is expanded and unstable on Huntington's disease chromosomes. The Huntington's Disease Collaborative Research Group. Cell. 1993; 72:971–83. [PubMed: 8458085]
3. DiFiglia M, Sapp E, Chase KO, et al. Aggregation of huntingtin in neuronal intranuclear inclusions and dystrophic neurites in brain. Science. 1997; 277:1990–3. [PubMed: 9302293]
4. Gutekunst CA, Li SH, Yi H, et al. Nuclear and neuropil aggregates in Huntington's disease: Relationship to neuropathology. J Neurosci. 1999; 19:2522–34. [PubMed: 10087066]
5. Dai Y, Dudek NL, Li Q, et al. Striatal expression of a calmodulin fragment improved motor function, weight loss, and neuropathology in the R6/2 mouse model of Huntington's disease. J Neurosci. 2009; 29:11550–9. [PubMed: 19759302]
6. DiFiglia M, Sena-Esteves M, Chase K, et al. Therapeutic silencing of mutant huntingtin with siRNA attenuates striatal and cortical neuropathology and behavioral deficits. Proc Natl Acad Sci U S A. 2007; 104:17204–9. [PubMed: 17940007]
7. Rodriguez-Lebron E, Denovan-Wright EM, Nash K, et al. Intrastriatal rAAV-mediated delivery of anti-huntingtin shRNAs induces partial reversal of disease progression in R6/1 Huntington's disease transgenic mice. Mol Ther. 2005; 12:618–33. [PubMed: 16019264]
8. Davies SW, Turmaine M, Cozens BA, et al. Formation of neuronal intranuclear inclusions underlies the neurological dysfunction in mice transgenic for the HD mutation. Cell. 1997; 90:537–48. [PubMed: 9267033]
9. Mangiarini L, Sathasivam K, Seller M, et al. Exon 1 of the HD gene with an expanded CAG repeat is sufficient to cause a progressive neurological phenotype in transgenic mice. Cell. 1996; 87:493–506. [PubMed: 8898202]
10. Miller TW, Messer A. Intrabody applications in neurological disorders: progress and future prospects. Mol Ther. 2005; 12:394–401. [PubMed: 15964243]
11. Naver B, Stub C, Moller M, et al. Molecular and behavioral analysis of the R6/1 Huntington's disease transgenic mouse. Neuroscience. 2003; 122:1049–57. [PubMed: 14643771]

12. Messer A, McLear J. The therapeutic potential of intrabodies in neurologic disorders: Focus on Huntington and Parkinson diseases. BioDrugs. 2006; 20:327–33. [PubMed: 17176119]
13. Lecerf JM, Shirley TL, Zhu Q, et al. Human single-chain Fv intrabodies counteract in situ huntingtin aggregation in cellular models of Huntington's disease. Proc Natl Acad Sci U S A. 2001; 98:4764–9. [PubMed: 11296304]
14. Miller TW, Zhou C, Gines S, et al. A human single-chain Fv intrabody preferentially targets amino-terminal Huntingtin's fragments in striatal models of Huntington's disease. Neurobiol Dis. 2005; 19:47–56. [PubMed: 15837560]
15. Murphy RC, Messer A. A single-chain Fv intrabody provides functional protection against the effects of mutant protein in an organotypic slice culture model of Huntington's disease. Brain Res Mol Brain Res. 2004; 121:141–5. [PubMed: 14969746]
16. Wolfgang WJ, Miller TW, Webster JM, et al. Suppression of Huntington's disease pathology in Drosophila by human single-chain Fv antibodies. Proc Natl Acad Sci U S A. 2005; 102:11563–8. [PubMed: 16061794]
17. Kvam E, Nannenga BL, Wang MS, et al. Conformational targeting of fibrillar polyglutamine proteins in live cells escalates aggregation and cytotoxicity. PLoS One. 2009; 4:5727.
18. Li H, Li SH, Cheng AL, et al. Ultrastructural localization and progressive formation of neuropil aggregates in Huntington's disease transgenic mice. Hum Mol Genet. 1999; 8:1227–36. [PubMed: 10369868]
19. Morton AJ, Lagan MA, Skepper JN, et al. Progressive formation of inclusions in the striatum and hippocampus of mice transgenic for the human Huntington's disease mutation. J Neurocytol. 2000; 29:679–702. [PubMed: 11353291]
20. Ehrnhoefer DE, Butland SL, Pouladi MA, et al. Mouse models of Huntington disease: variations on a theme. Dis Model Mech. 2009; 2:123–9. [PubMed: 19259385]
21. Saudou F, Finkbeiner S, Devys D, et al. Huntingtin acts in the nucleus to induce apoptosis but death does not correlate with the formation of intranuclear inclusions. Cell. 1998; 95:55–66. [PubMed: 9778247]
22. Arrasate M, Mitra S, Schweitzer ES, et al. Inclusion body formation reduces levels of mutant huntingtin and the risk of neuronal death. Nature. 2004; 431:805–10. [PubMed: 15483602]
23. Yamamoto A, Lucas JJ, Hen R. Reversal of neuropathology and motor dysfunction in a conditional model of Huntington's disease. Cell. 2000; 101:57–66. [PubMed: 10778856]
24. Wang CE, Tydlacka S, Orr AL, et al. Accumulation of N-terminal mutant huntingtin in mouse and monkey models implicated as a pathogenic mechanism in Huntington's disease. Hum Mol Genet. 2008; 17:2738–51. [PubMed: 18558632]
25. Southwell AL, Ko J, Patterson PH. Intrabody gene therapy ameliorates motor, cognitive, and neuropathological symptoms in multiple mouse models of Huntington's disease. J Neurosci. 2009; 29:13589–602. [PubMed: 19864571]
26. Gu X, Greiner ER, Mishra R, et al. Serines 13 and 16 are critical determinants of full-length human mutant huntingtin induced disease pathogenesis in HD mice. Neuron. 2009; 64:828–40. [PubMed: 20064390]
27. Davidson BL, Breakefield XO. Viral vectors for gene delivery to the nervous system. Nat Rev Neurosci. 2003; 4:353–64. [PubMed: 12728263]
28. Reimsnider S, Manfredsson FP, Muzyczka N, et al. Time course of transgene expression after intrastriatal pseudotyped rAAV2/1, rAAV2/2, rAAV2/5, and rAAV2/8 transduction in the rat. Mol Ther. 2007; 15:1504–11. [PubMed: 17565350]
29. Dodiya HB, Bjorklund T, Stansell J 3rd, et al. Differential transduction following basal ganglia administration of distinct pseudotyped AAV capsid serotypes in nonhuman primates. Mol Ther. 2010; 18:579–87. [PubMed: 19773746]
30. Wang C, Wang CM, Clark KR, et al. Recombinant AAV serotype 1 transduction efficiency and tropism in the murine brain. Gene Ther. 2003; 10:1528–34. [PubMed: 12900769]
31. Burger C, Gorbatyuk OS, Velardo MJ, et al. Recombinant AAV viral vectors pseudotyped with viral capsids from serotypes 1, 2, and 5 display differential efficiency and cell tropism after delivery to different regions of the central nervous system. Mol Ther. 2004; 10:302–17. [PubMed: 15294177]

32. Giampa C, Patassini S, Borreca A, et al. Phosphodiesterase 10 inhibition reduces striatal excitotoxicity in the quinolinic acid model of Huntington's disease. Neurobiol Dis. 2009; 34:450–6. [PubMed: 19281846]

33. Ferrante RJ, Kowall NW, Beal MF, et al. Selective sparing of a class of striatal neurons in Huntington's disease. Science. 1985; 230:561–3. [PubMed: 2931802]

34. Bortvedt SF, McLear JA, Messer A, et al. Cystamine and intrabody co-treatment confers additional benefits in a fly model of Huntington's disease. Neurobiol Dis. 2010; 40:130–34. [PubMed: 20399860]

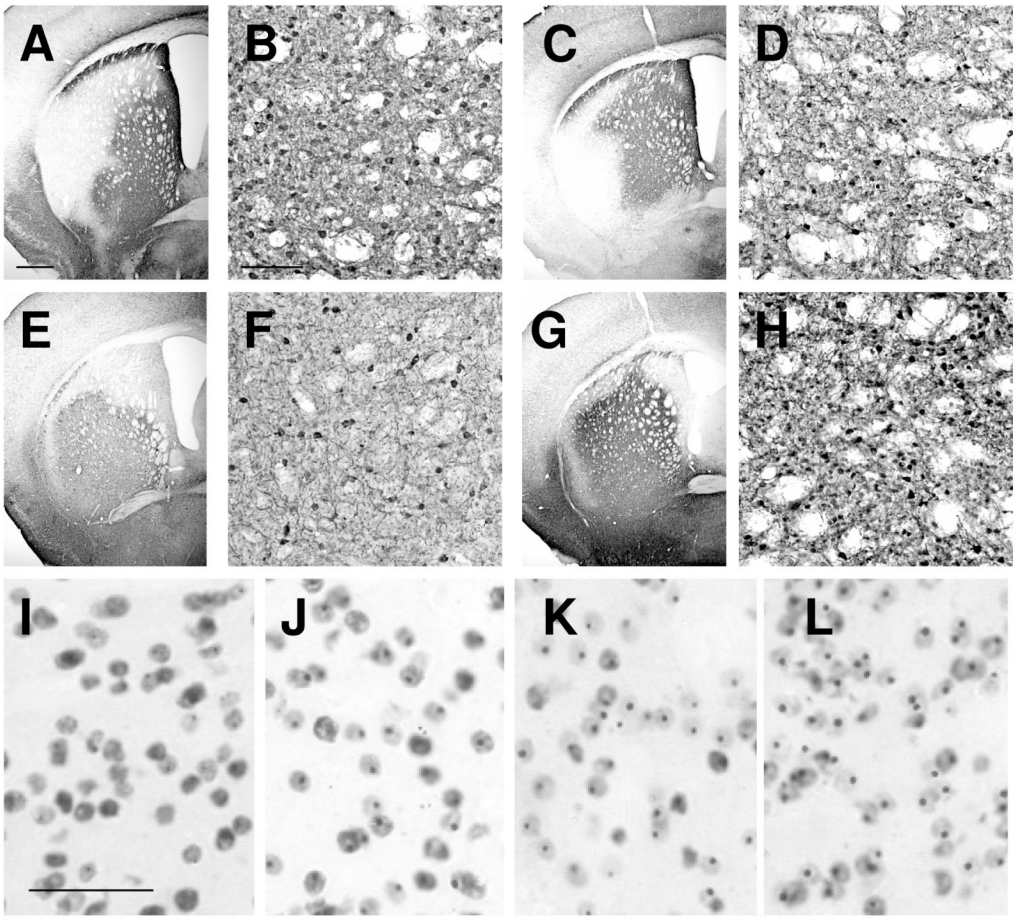

Figure 1.

Intrastriatal injections of AAV2/1 scFv-C4 produce robust expression of C4 in both young and old B6.HDR6/1 (HD) mouse brains. Low- and high-magnification views of sections from wild type (wt) (**A, B**) and HD (**C-H**) mouse brains immunostained for the hemagglutinin tag demonstrate that comparable transduction occurs in young and old HD and wt brains. (**A-D**) Mice injected at 5 weeks, killed at 24 weeks. (**E, F**) HD mouse injected at 16 weeks, killed at 26 weeks. (**G, H**) HD mouse injected at 24 weeks, killed at 34 weeks. (**I-L**) Mutant htt immunostaining (EM48 antibody) at 8 weeks (**I**), 16 weeks (**J**), 20 weeks (**K**), and 24 weeks (**L**) of age. Scale bar in **A** = 500 μm (for **A, C, E, G**); Bar in **B** = 100 μm (for **B, D, F, H**); Bar in **I** = 50 μm (for **I-L**).

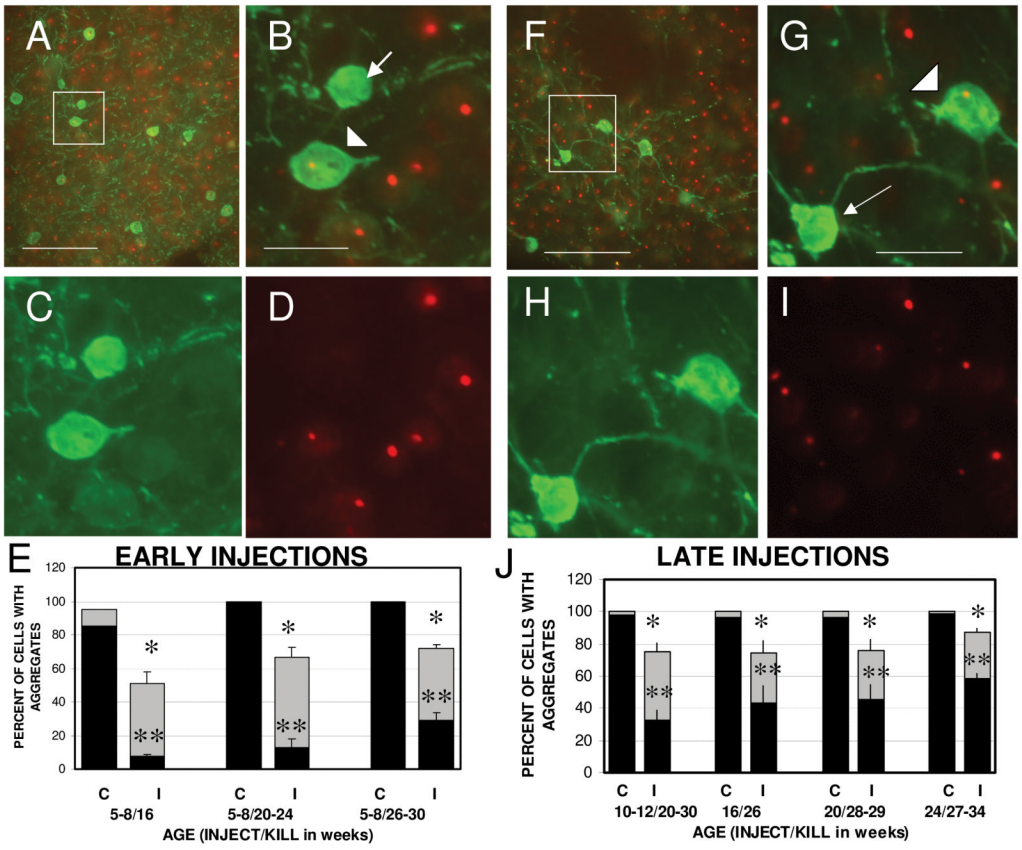

Figure 2.

scFv-C4 expression reduces the size and frequency of mhtt aggregates in striatal neurons after AAV2/1 scFv-C4 injections. Panels **A-E** show results from B6.HDR6/1 (HD) mice injected at 5 to 8 weeks of age; panels **F-J** from mice injected at 10 to 24 weeks of age. (**A-D**) Fluorescent images illustrating a representative a field from 23- week HD striatum (after scFv-C4 injection at 6 weeks) showing hemagglutinin (HA)-labeled (transduced) neurons (green), and EM48 immunostaining (red) to visualize mhtt aggregates. The merged image (**B**, higher magnification of box in **A**) illustrates transduced neurons with no aggregates (arrow) or smaller aggregates (arrowhead) than seen in non-transduced neurons in the vicinity. (**C, D**) Separate HA (**C**) and EM48 (**D**) immunostaining. (**E**) Quantification of presence of mhtt aggregates in striatal neurons from injected HD mice grouped by age at time of sacrifice (n = 4 each at 16 weeks and at 20 to 24 weeks, and n = 6 at 26 to 30 weeks). Each pair of bars represents the percentage of cells exhibiting aggregates in non-transduced cells (left side; **C**, control) and transduced (HA-immunoreactive) cells (right side; I, intrabody). The black portion of each bar represents large aggregates; the total height of each bar indicates the total percentage of cells that contain aggregates. Bars = mean ± SEM. ANOVA revealed a significant main effect of intrabody on total aggregate expression (*) ($F = 653.67$, $p < 0.0001$) and the presence of large aggregates (**) ($F = 170.27$, $p < 0.0001$). There was also a significant effect of age at sacrifice for both total ($F = 5.28$, $p < 0.05$) and large ($F = 9.48$, $p < 0.002$) aggregates, and a significant interaction between intrabody effect (total and large) and age at sacrifice ($P<0.02$). F-I: Fluorescent images of a representative field from 26-week HD striatum (after scFv-C4 injection at 16 weeks). (**J**) Quantification of mhtt aggregates in striatal neurons after AAV2/1 scFv-C4 injections at older ages. Animals were grouped by age at time of injection: 10 to 12 weeks (n = 6, killed at 20 to 30 weeks), 16 weeks (n = 3, killed at 26 weeks), 20 weeks (n = 3, killed at 28 to 29

weeks), 24 weeks (n = 5, killed at 27 to 34 weeks). To assess the statistical significance of the age at which the injections were made, we performed ANOVA on counts from all mice killed at 26 weeks of age or older; that grouping includes the right-most set of bars from E (injected at 5-8 weeks of age). This revealed a significant main effect of intrabody on total aggregate expression (*)($F = 92.1$, $p < 0.0001$), and the presence of large aggregates (**) ($F = 305.08$, $p < 0.0001$). There was also a significant main effect of age of injection for large aggregates only ($F = 3.78$, $p < 0.05$), as well as an interaction between intrabody and age of injection ($F = 3.43$, $p < 0.05$), reflecting diminishing efficacy in older mice. (**C, D, H, I**) Separate HA (**C, H**) and EM48 (**D, I**) immunostaining for comparison to **B** and **G**. Scale bars: 100 μm in **A** and **F**, 25 μm in **B-D**, and **G-I**.